Atomic Force Microscope Imaging of Phospholipid Bilayer Degradation by Phospholipase A_2

Michel Grandbois, Hauke Clausen-Schaumann, and Hermann Gaub
Lehrstuhl für Angewandte Physik, Ludwig Maximilians Universität München, 80799 Munich, Germany

ABSTRACT We have investigated the time course of the degradation of a supported dipalmitoylphosphatidylcholine bilayer by phospholipase A_2 in aqueous buffer with an atomic force microscope. Contact mode imaging allows visualization of enzyme activity on the substrate with a lateral resolution of less than 10 nm. Detailed analysis of the micrographs reveals a dependence of enzyme activity on the phospholipid organization and orientation in the bilayer. These experiments suggest that it is possible to observe single enzymes at work in small channels, which are created by the hydrolysis of membrane phospholipids. Indeed, the measured rate of hydrolysis of phospholipids corresponds very well with the enzyme activity found in kinetic studies. It was also possible to correlate the number of enzymes at the surface, as calculated from the binding constant to the number of starting points of the hydrolysis. In addition, the width of the channels was found to be comparable to the diameter of a single phospholipase A_2 and thus further supports the single-enzyme hypothesis.

INTRODUCTION

The atomic force microscope (AFM) has become a well-established instrument for investigating the structure and mechanical properties of biological material (Müller et al., 1996; Radmacher et al., 1992, 1995; Rief et al., 1997). The possibility of imaging the sample in buffer solution makes possible the characterization of biological material under native conditions. Recently single enzyme activity has been directly observed (Radmacher et al., 1994), demonstrating the potential of atomic force microscopy for investigating the dynamics of biological processes on the molecular level.

Phospholipase A_2 (PLA_2) is an interfacially activated enzyme that catalyzes regio- and stereospecific hydrolysis of the sn-2 acyl ester linkage of sn-3-glycero-phospholipids, producing fatty acid and lysophospholipid as reaction products. It is well recognized that PLA_2 activity at lipid membrane interfaces (i.e., vesicles, multilamellar dispersions, monolayers at the air-water interface, and supported bilayers) is much higher than in isotropically dispersed phospholipids. The activity of this enzyme varies accordingly with the physicochemical properties of the interface (Dennis, 1983). It was found that the enzyme activity is also dependent on the organization of phospholipids in the membrane (Burack and Biltonen, 1994). Several studies have proposed that the presence of defects in the bilayer structure may act as starting points for the enzyme activity (Grainger et al., 1989; Grandbois et al., 1996; Vernon and Bell, 1992). In addition, a more general concept considering different phospholipid organizations was proposed to explain the different activity of PLA_2 for different substrates. For example, PLA_2 exhibits higher activity for micelles in comparison to planar bilayers, and its activity reaches a maximum in the phase transition region of dipalmitoylphosphatidylcholine (DPPC) (Bell and Biltonen, 1989; Lichtenberg et al., 1986; op den Kamp et al., 1975; van Hoogevest et al., 1984). Several methods can be used to follow the activity of this enzyme. These include monitoring the surface area of a monolayer at the air-water interface (Verger and Rivière, 1987), pH titration (Reynolds et al., 1991), chromatography (Blank and Snyder, 1991), fluorescence spectroscopy (Jain and Maliwal, 1993), fluorescence microscopy (Grainger et al., 1989), ellipsometry (Speijer et al., 1996), quartz microbalance (Okahata and Ebara, 1992), x-ray scattering (Dahmen-Levison, personal communication), and infrared spectroscopy (Gericke and Hühnerfuss, 1994). Recently, epifluorescence microscopy was used to image the degradation of phospholipid monolayers with a micrometer resolution (Grainger et al., 1989, 1990; Grandbois et al., 1996; Maloney et al., 1995). In these studies the authors have observed the time course of the hydrolysis of solid phospholipid domains of a lipid monolayer in the phase transition. They have also observed the formation of enzyme domains at the air-water interface simultaneously with the hydrolysis of the solid phospholipid domains. However, the low resolution of the epifluorescence microscope has made the investigation of the molecular degradation process of the phospholipid monolayer inaccessible. In the present study, we report the imaging of the degradation process of a supported DPPC bilayer in the gel phase with a lateral resolution of less than 10 nm by AFM. Thorough analysis of the data provides information about the behavior of the enzyme on gel phase phospholipid bilayers at a nanoscopic scale. In addition, experimental evidence suggests that it is possible to observe single enzyme activity in the narrow channels formed in the membrane in the first minutes of the bilayer hydrolysis.

Received for publication 14 July 1997 and in final form 6 February 1998.

Address reprint requests to Dr. Hermann Gaub, Lehrstuhl für Angewandte Physik, Ludwig Maximilians Universität München, Amalienstrasse 54, 80799 Munich, Germany. Tel.: 49-89-2180-3172; Fax: 49-89-2180-2050; E-mail: gaub@physik.uni-muenchen.de.

© 1998 by the Biophysical Society

0006-3495/98/05/2398/07 $2.00

MATERIALS AND METHODS

Bee venom PLA_2 0,136 U/mg (Sigma-Aldrich Chemie, D-82039 Deisenhofen, Germany) and DPPC (Avanti Polar Lipids, Alabaster, AL) were

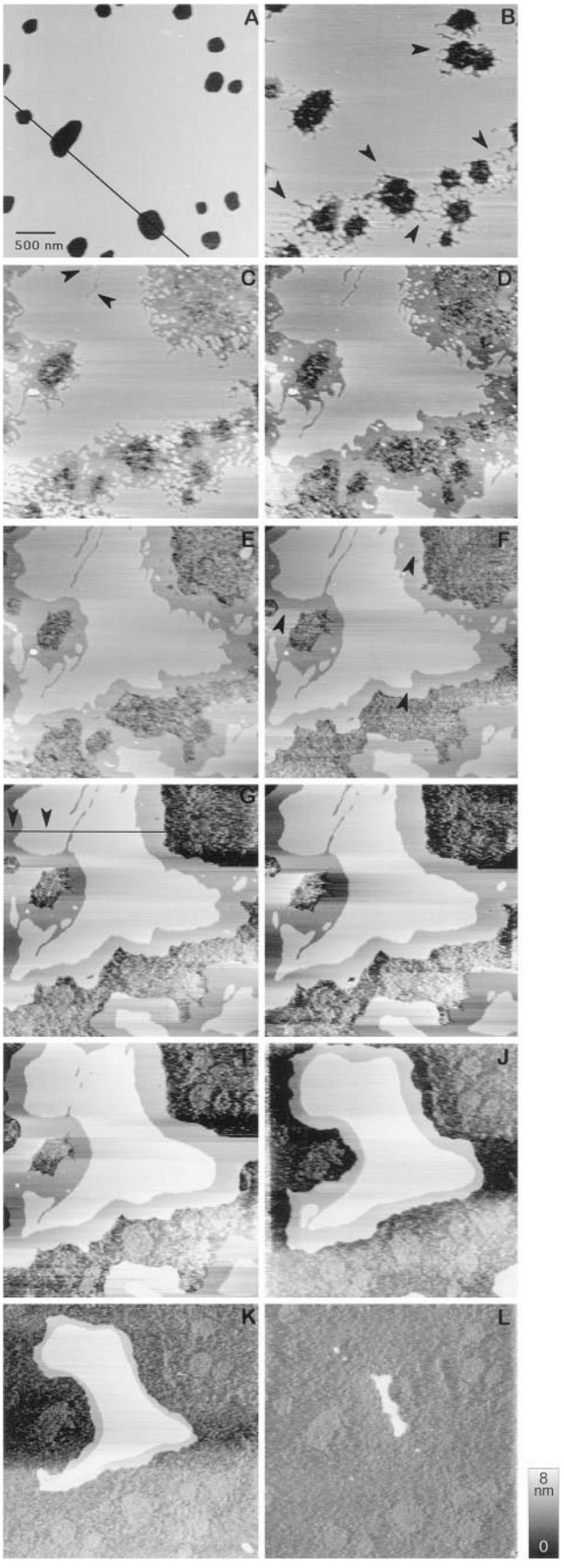

FIGURE 1 AFM images of the time sequences of the hydrolysis of a mica-supported DPPC bilayer by PLA_2. (*A*) Before PLA_2 injection, and (*B*) 2 min, (*C*) 4 min, (*D*) 6 min, (*E*) 9 min, (*F*) 12 min, (*G*) 14 min, (*H*) 17 min, (*I*) 30 min, (*J*) 50 min, (*K*) 80 min, (*L*) 140 min after PLA_2 injection. Buffer composition: 100 mM NaCl, 5 mM $CaCl_2$, 10 mM Tris, pH 8.9. Imaging parameters: raw data baseline corrected, constant force ($\leq$ 0.5 nN), EBD tip (35 mN/m), 6.1 lines/s scan speed.

used without further purification. NaCl (Sigma Ultra >99.5%), $CaCl_2$ (Sigma Ultra >99%), and trihydroxymethylaminomethane (Tris) (Sigma, >99.5%) were also used as received. The water used was filtered on a Millipore Milli-Q Plus system. Its resistivity and surface tension were higher than 18 MΩ/cm and 71 mN/m, respectively.

Supported DPPC bilayers were prepared with a home-built Langmuir trough according to the procedure of Tamm and McConnell (1985), using freshly cleaved mica as a solid support. Phospholipid monolayers were spread on pure Millipore water from a DPPC chloroform solution (2 mg/ml). The vertical transfer of the first layer was performed at 50 μm/s, and the film was allowed to dry for 15 min before the horizontal transfer of the second layer. The surface pressure of the DPPC monolayer was kept at 35 mN/m and the temperature at 25°C for both transfers.

The supported bilayer was then transferred to the fluid cell of the AFM (Nanoscope IIIa, Digital Instruments, Santa Barbara, CA). A silicon o-ring was used to keep the supported bilayer immersed in water after the LB transfer and to seal the AFM fluid cell. To minimize adhesion forces as well as the contamination of the tip by hydrolysis products, we used a silicon nitride cantilever (Digital Instruments) with a 2-μm-long electron beam-deposited tip (EBD tip) on top of the 4-μm silicon nitride pyramid (Wendel et al., 1995). Cantilever calibration (Florin et al., 1995) yielded a spring constant of 35 mN/m. The piezo scanner had been calibrated against a grid of known dimensions. The supported bilayer was imaged in the constant-force mode, with a loading force of less than 0.5 nN, at a scan rate of 6 Hz (lines per second). Trace and retrace images were compared to correct for friction-induced height artifacts. All experiments were conducted at room temperature (25°C). The supported lipid bilayer was incubated in the AFM fluid cell with buffer solution (5 mM $CaCl_2$, 100 mM NaCl, and 10 mM Tris, pH 8.9) containing no PLA_2 for 30 min before the first image was recorded. Hydrolysis of the bilayer was then initiated by injecting the same buffer containing 0.26 μM bee venom PLA_2 into the fluid cell.

The histogram shown in Fig. 5 was obtained from 93 angles measured at points were the direction of a single channel changes or at branches between two channels (Fig. 1, *B* and *C*). The line shown in Fig. 7 was created by scanning the supported bilayer over the same line for 5 min in the buffer solution (5 mM $CaCl_2$, 100 mM NaCl, and 10 mM Tris, pH 8.9) in the presence of 0.13 μM PLA_2. The loading force was set to 5 nN and the scan rate to 28 Hz. Then scanning parameters were set back to their initial values (see previous paragraph) to allow imaging of the supported bilayer. As a control, an experiment was performed under the same conditions in the absence of PLA_2.

RESULTS AND DISCUSSION

Supported lipid membranes in the gel phase can be stably imaged with the AFM (Hui et al., 1995; Mou et al., 1994a,b). Fig. 1 *A* shows an LB film of DPPC transferred on mica (see Materials and Methods for details), in which the phospholipids are organized in a gel-phase unilamellar bilayer. The dark regions are holes in the film, with an average size of 260 nm. The height difference between the lipid film (*bright regions*) and the mica substrate (*dark regions*) was found to be 6.0 $\pm$ 0.2 nm (see Fig. 2 *A*). This value is in good agreement with x-ray diffraction (Cevc and Marsh, 1987) as well as AFM data (Shao and Yang, 1995),

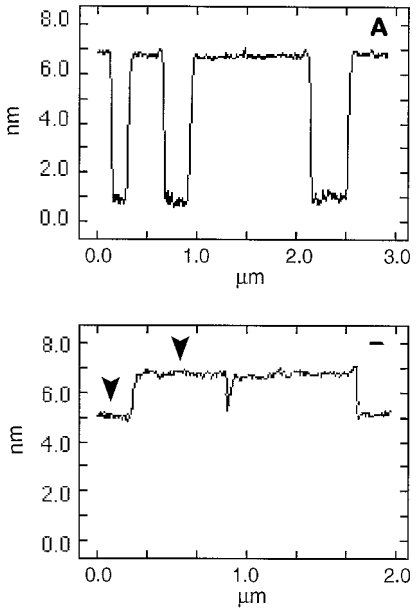

FIGURE 2 (*A*) Profile along the line drawn in Fig. 1 *A*. The height difference (6.0 ± 0.2 nm) between the arrows corresponds to the height of the supported DPPC bilayer. (*B*) Profile along the line drawn in Fig. 1 *G*. The height difference (1.5 ± 0.2 nm) between the arrows corresponds to the height difference between a nonhydrolyzed bilayer and a bilayer with the upper leaflet consisting of hydrolysis products

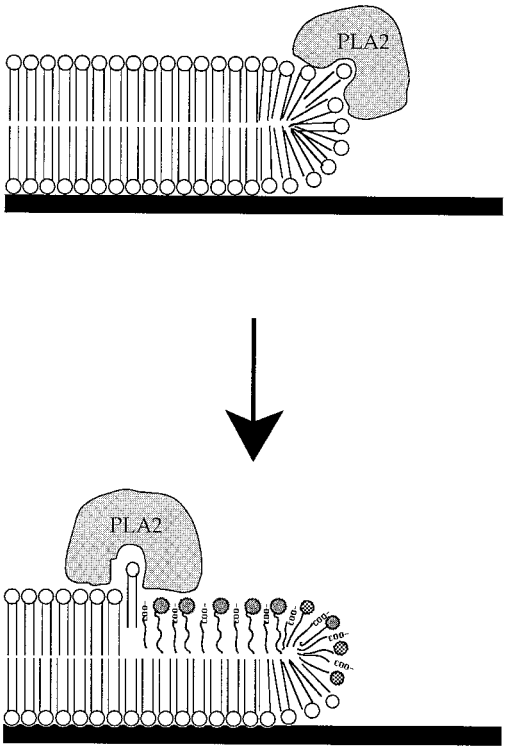

FIGURE 3 Model for the organization and the hydrolysis by PLA_2 of the phospholipids at the edge of the bilayer defects.

and indicates the unilamellar bilayer organization of the adsorbed phospholipids.

Fig. 1, *A–L*, presents a typical time sequence of DPPC bilayer degradation upon phospholipid hydrolysis by PLA_2. Two minutes after the PLA_2 injection into the fluid cell, numerous narrow channels (see *arrows* in Fig. 1 *B*) resulting from the enzyme activity can be observed in the bilayer. Because the enzymes hydrolyze the DPPC gel phase at a very low rate (Kensil and Dennis, 1979; op den Kamp et al., 1975), the formation of the channels can start only at the border of the membrane, i.e., at the rim of the holes in Fig. 1 *A*, where the phospholipids are not well packed. In the uniform DPPC gel phase region, where the phospholipids are well organized, no degradation of the membrane was observed. The high curvature of the molecular organization of the phospholipids at the border of the bilayer (see model in Fig. 3) may explain the preference of the enzyme for these regions: the curvature prevents the crystalline packing of the lipids and thus increases the accessibility of the cleavage site, the glycerol backbone of the phospholipids, to the enzyme. This observation is in good agreement with studies (Bell and Biltonen, 1989; Lichtenberg et al., 1986; op den Kamp et al., 1975; van Hoogevest et al., 1984) that show an enhanced enzyme activity in the liquid/gel phase transition of DPPC, where the packing shows a maximum of heterogeneity. Moreover, for DPPC monolayers in the phase transition, it has been shown (Grainger et al., 1989; Grandbois et al., 1996) that the hydrolysis of the phospholipid solid domains starts only at particular points, corresponding to defects at the liquid-solid phase boundary.

Two minutes after the injection of PLA_2 (Fig. 1 *B*), the growth of the channels is clearly visible. A closer look (see Fig. 4) also shows frequent changes in channel orientation and the branching of numerous channels, leading to fragmentation of the membrane. Analysis of these images provides insight into the mechanism of PLA_2 activity. An angular distribution of the different directions of single channels or between two branches shows a pronounced maximum close to 120° (Fig. 5 *A*). It is tempting to relate this particular angle to the local hexagonal packing of the DPPC bilayer in the gel phase (Cevc and Marsh, 1987). This suggests that the enzyme is sensitive to the crystal axes of the DPPC bilayer. The enzyme may sense the orientation of the lipids directly, or it may act as an amplifier for defects that are already present in the membrane. PLA_2 may thus be used as a tool to investigate the effect of different ions or molecules, interacting either with polar headgroup or acyl chains, on the packing of phospholipids.

Channel formation in the DPPC bilayer upon PLA_2 injection raises the question of whether we observe single enzyme activity. In fact, the formation of a particular channel may be due to the simultaneous action of several enzymes or to the action of a single enzyme. A detailed analysis of the images strongly supports the hypothesis of a single enzyme at work in each channel. In Fig. 1 *B* (see also Fig. 4 for more details) it is possible to identify numerous small channels with a width of ~15 ± 3 nm, corresponding to 22 phospholipids. This value takes into account the convolution of the tip and surface geometry. If we assume

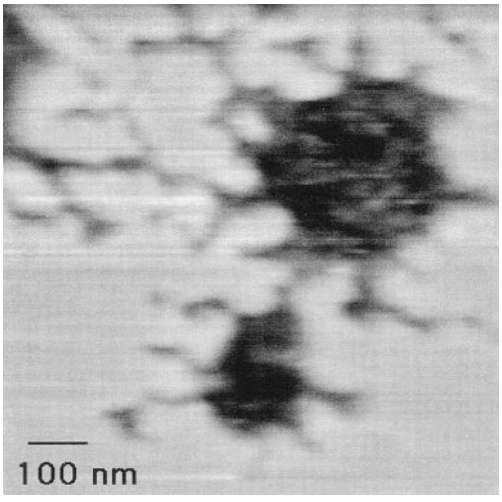

FIGURE 4 Closer view of Fig. 1 *B*, showing the numerous small channels starting at the edge of defects present in the supported bilayer. In this image it is possible to distinguish several angle with values close to 120°.

a cross-sectional diameter for the PLA_2 of 5 nm (Verger et al., 1973), it seems very improbable that more than one enzyme is responsible for the formation of a single channel. This interpretation is corroborated by calorimetric data (Lichtenberg et al., 1986), which shows that one PLA_2 molecule interacts with ~40 phospholipids on its binding site.

The upper part of Fig. 1, *C–F* (see *arrows*), reveals the simultaneous growth of two adjacent channels growing in the same direction at the same speed. In Fig. 1 *E*, however, the left channel stops growing, whereas the right one continues to grow in the same direction until an already hydrolyzed region of the membrane is reached. This observation has been quantified in Fig. 6 by plotting the increase of the channel lengths versus time. The plateau seen in these two curves clearly shows that the left channel (*black line*) stops growing 9 min after the enzyme injection, whereas there is still a variation in length for the right one (*gray line*). This observation further supports the single enzyme hypothesis. In fact, if there were several enzymes present in each channel, it should be highly unlikely that the enzymes present in the left channel become simultaneously inactive or detached, while all of the enzymes in the right channel continue to hydrolyze the membrane. In addition, the first linear ramp of the two curves was used to obtain an estimate of the number of lipids hydrolyzed per second in both channels. For an average channel width of 40 nm, we obtain a rate of hydrolysis of 102 and 108 ± 30 molecules/s per enzyme for the left and right channels, respectively. Furthermore, the rate of hydrolysis of 66 well-defined channels growing from Fig. 1 *A* to Fig. 1 *B* was calculated: the obtained value (88 ± 30 molecules/s per enzyme) was found to be very close to the one obtained in the previous calculation for the two adjacent channels. This shows that it is possible to estimate the rate of hydrolysis with an acceptable precision, even if two different sets of pictures are compared. These enzyme activity values as calculated from the AFM images are on the same order of magnitude as the known value of PLA_2 activity (see Materials and Methods), which is 230 molecules/s per enzyme for a phosphatidylcholine lipid dispersion and further corroborates the single enzyme hypothesis.

Additional support for the single enzyme hypothesis may be derived from the number of channels that are present at

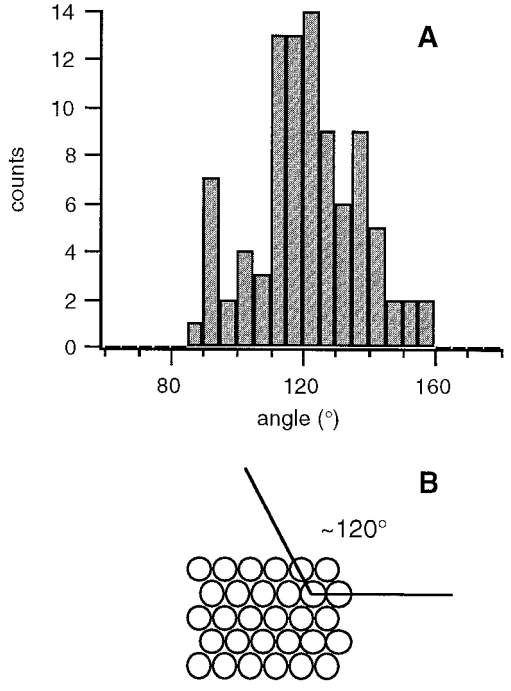

FIGURE 5 (*A*) Histogram of the angles between two directions of a single channel or between two branches calculated from Fig. 1 *B*. This histogram shows a maximum centered at 120°. (*B*) Schematic of the crystal axes of DPPC in the solid phase.

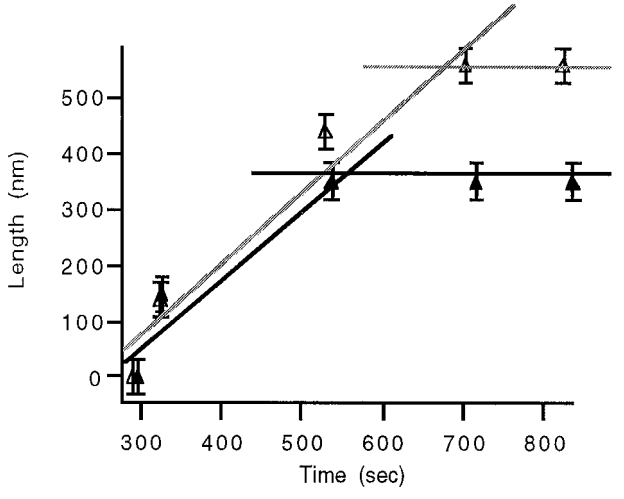

FIGURE 6 Increase of the length versus time for the two channels marked from Fig. 1 *C* to Fig. 1 *G*. The activity of the enzyme was calculated from the slope of the fitted lines. The beginning of the plateau corresponds to the time at which PLA_2 became inactive. The black and the gray lines correspond to the left and the right channel, respectively.

the beginning of the hydrolysis. If single enzymes are responsible for the formation of individual channels, then the number of channels starting immediately after the beginning of the hydrolysis (Fig. 1 *B*) should not be significantly smaller than the number of enzymes bound to the membrane. Because we observed that hydrolysis starts only at the border of the membrane, we used a 25-nm-wide strip around the bilayer defects of Fig. 1 *A*, and a simple binding model (Biltonen et al., 1991) with a surface binding constant of 10^{-4} M (Bell and Biltonen, 1989; Jain et al., 1991) to calculate this number. It should be noted that 25 nm represents an upper estimate for the border area that is accessible to the enzyme. This calculation gives a value of 42 molecules for all the edge area in Fig. 1 *A*. However, in Fig. 1 *B* it is possible to count at least 100 different channels surrounding the defects in the supported bilayer. This, again, suggests that it is unlikely that more than one enzyme is responsible for the formation of a single channel.

From Fig. 1 *E* to the end, the degradation of the DPPC bilayer seems to follow a different pattern. The hydrolysis becomes slower and the numerous small channels tend to anneal and disappear. The decrease in the hydrolysis speed has been quantified in Fig. 7 by plotting the percentage of the DPPC bilayer hydrolyzed on a logarithmic scale versus time. One can observe in this figure two well-defined phases in the hydrolysis of the bilayer with an inflexion (see *mark*) corresponding to the extent of hydrolysis at Fig. 1 *E*. The first part of the graph corresponds to the beginning of the hydrolysis of the DPPC bilayer containing no hydrolysis products as impurities. The drastic change in the hydrolysis speed is concomitant with the annealing of the small channels and the appearance of the gray region surrounding the DPPC bilayer (see *arrows* in Fig. 1 *F*). Because the channels contain hydrolysis products (lysophosphatidylcholine and palmitic acid) that do not form stable films (Maloney et al., 1995; Patil et al., 1973), it is very likely that the annealing is due to the reorganization of nonhydrolyzed DPPC, after the solubilization of the hydrolysis products. The height difference between the white and gray regions of ~1.5 nm (Fig. 2 *B*) can be associated with the presence of hydrolysis products in the gray region of the image. Thus the gray region should be composed of a first intact DPPC layer, in close contact with the mica substrate, and a second layer composed of hydrolysis products. From Fig. 1 *E* to Fig. 1 *L* we observe the simultaneous degradation of the white and gray regions of the bilayer. The hydrolysis of the gray region implies the transfer of lipids from the first layer of the supported membrane to the upper layer. This transfer is believed to occur at the border of the lipid bilayer. The rate of this transfer, together with the reduced concentration of DPPC at the border, should limit the speed of the overall hydrolysis process observed from Fig. 1 *E* to Fig. 1 *L* (see also Fig. 7). This experimental evidence suggests that hydrolysis products have an important influence on the enzyme activity on the supported DPPC bilayer. Moreover, it is impossible to distinguish in Fig. 1, *E–L*, the contribution of the solubilization of the DPPC bilayer by the hydrolysis products from the overall hydrolytic process. This solubilization should be related to the stability of the supported bilayer. Separate experiments with phosphatidylcholine of different chain lengths are currently being conducted to clarify this point. It should be noted that it was impossible to observe the formation of the PLA_2 domains observed by Grainger et al. (1990) for the degradation of DPPC monolayer in the phase transition in this experiment. The phase transition of the DPPC monolayer is perhaps a sine qua non for the PLA_2 domain formation. In our experiment the LB film was transferred at high surface pressure to form a supported bilayer in the gel phase.

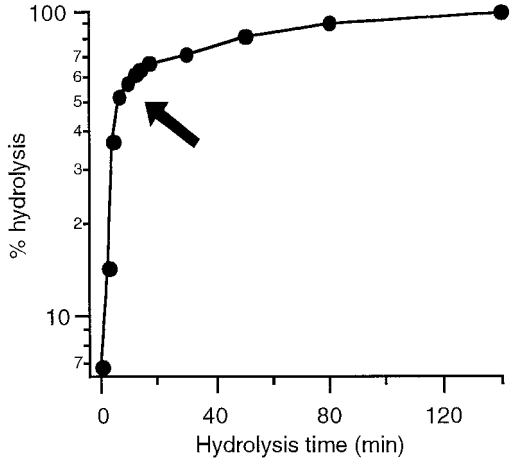

FIGURE 7 Percentage of the DPPC bilayer hydrolyzed by PLA_2 on a logarithmic scale versus time. The percentages were calculated from the area occupied by the DPPC bilayer at different times.

Because the activity of PLA_2 depends on the heterogeneity of the phospholipid organization, it was tempting to use the microscope tip to induce perturbation in the uniform gel phase region of the DPPC bilayer. Fig. 8 *A* shows a line in a DPPC bilayer obtained by increasing the loading force and the scan speed of the AFM tip in the presence of PLA_2 (see Materials and Methods for details). The height difference obtained from the profile (Fig. 8 *B*) gives a value of 1.5 nm between the line (*gray region*) and the white region. This height difference is comparable to the one found in Fig. 1 *G* between the gray and white regions and can therefore be attributed to the formation of a second layer of hydrolysis products. This finding directly demonstrates the selectivity of the PLA_2 for phospholipid packing defects. In this experiment the defect was mechanically induced at will by the AFM tip. It should be noted that it was not possible to scratch a line under the same experimental conditions in the absence of PLA_2. This very simple experiment also opens the possibility of enzyme-controlled nanolithography in molecular thin films. In fact, it should be possible to create specific motifs in the surface with the AFM tip in the presence of enzyme. The chelating of calcium or the addition of an enzyme inhibitor should allow researchers to stop the enzymatic process, avoiding further hydrolysis of the surface.

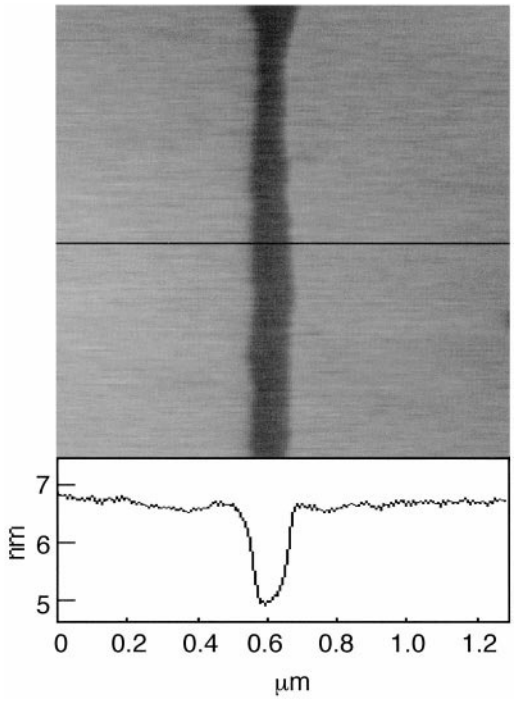

FIGURE 8 (*A*) Image of the line induced in the supported DPPC bilayer by scanning a region at a high scan rate (20 Hz) and high loading force (5 nN) in the presence of PLA_2. (*B*) Profile across of this line showing a height difference of 1.6 ± 0.2 nm. Same buffer as in Fig. 5.

CONCLUSIONS

In this article the AFM was used to investigate the hydrolysis of a supported bilayer by the lipolytic enzyme PLA_2. It was possible to get direct visual evidence of the dependence of enzyme activity on the substrate organization. We demonstrated that the enzyme hydrolyzes the supported bilayer only in regions where defects are present and that it exhibits a preference for the orientation of the lipid lattice. Moreover, a great deal of experimental evidence suggests that the formation of well-defined channels is due to the action of single enzymes. This opens the possibility of studying the activity of a single enzyme under different conditions believed to modulate the bilayer organization. Finally, the AFM tip was used to induce perturbation in the upper layer of the supported bilayer in such a way that only a well-defined membrane region was hydrolyzed by the enzyme. It is tempting to propose this experimental protocol as a new tool for nanolithography.

We thank Manfred Radmacher and Julio Fernandez for stimulating discussion, Martin Benoit for tip preparation, and Patrick Schluz-Vanheyden for cantilever calibration.

MG acknowledges the postdoctoral fellowship from the Natural Science and Engineering Research Council of Canada. This work was supported by the Deutsche Forschungsgemeinschaft.

REFERENCES

Bell, J. D., and R. L. Biltonen. 1989. Thermodynamic and kinetic studies of the interaction of vesicular dipalmitoylphosphatidylcholine with *Agkistrodon piscivorus piscivorus* phospholipase A_2. *J. Biol. Chem.* 264:225–230.

Biltonen, R. L., B. K. Lathrop, and J. D. Bell, 1991. Thermodynamics of Phospholipase A_2-Ligand Interactions. Academic Press, New York.

Blank, M. L., and F. Snyder. 1991. Chromatographic Analysis of Phospholipase Reaction Products. Academic Press, New York.

Burack, W. R., and R. L. Biltonen. 1994. Lipids bilayer heterogeneities and modulation of phospholipase A_2 activities. *Chem. Phys. Lipids.* 1994: 209–222.

Cevc, G., and D. Marsh. 1987. Phospholipid Bilayers. Wiley, New York.

Dennis, E. A. 1983. Phospholipases: The Enzymes. Academic Press, New York.

Florin, E. L., M. Rief, H. Lehmann, M. Ludwig, C. Dornmair, V. T. Moy, and H. E. Gaub. 1995. Sensing specific molecular interactions with the atomic force microscope. *Biosens. Bioelectron.* 10:895–901.

Gericke, A., and H. Hühnerfuss. 1994. IR reflection absorption spectroscopy: a versatile tool for studying interfacial enzymatic processes. *Chem. Phys. Lipids.* 74:205–210.

Grainger, D. W., A. Reichert, H. Ringsdorf, and C. Salesse. 1989. An enzyme caught in action: direct imaging of hydrolytic function and domain formation of phospholipase A_2 in phosphatidylcholine monolayers. *FEBS Lett.* 252:73–82.

Grainger, D. W., A. Reichert, H. Ringsdorf, and C. Salesse. 1990. Hydrolytic action of phospholipase A_2 in monolayer phase transition region: direct observation of enzyme domain formation using fluorescence microscopy. *Biochim. Biophys. Acta.* 1023:365–379.

Grandbois, M., C. Salesse, and J. Dufourcq. 1996. Study of the synergistic action of phospholipase A2 and melittin in the hydrolysis of phospholipid monolayers. *Thin Solid Films.* 284,285:743–747.

Hui, S. W., R. Viswanathan, J. A. Zasadzinski, and J. N. Israelachvili. 1995. The structure and stability of phospholipid bilayers by atomic force microscopy. *Biophys. J.* 68:171–178.

Jain, M. K., and B. P. Maliwal. 1993. Spectroscopic properties of the states of pig pancreatic phospholipase A_2 at interfaces and their possilble molecular origin. *Biochemistry.* 32:11838–11846.

Jain, M. K., G. Ranadive, B.-Z. Yu, and H. M. Verheij. 1991. Interfacial catalysis by phospholipase A_2: monomeric enzyme is fully catalytically active at the bilayer interface. *Biochemistry.* 30:7330–7340.

Kensil, C. R., and E. A. Dennis. 1979. Action of cobra venom phospholipase A_2 on the gel and liquid crystalline states of dimyristoyl and dipalmitoyl phosphatidylcholine vesicles. *J. Biol. Chem.* 254: 5843–5848.

Lichtenberg, D., G. Romero, M. Menashe, and R. L. Biltonen. 1986. Hydrolysis of dipalmitoylphosphatidylcholine large unilamellar vesicles by porcine pancreatic phospholipase A_2. *J. Biol. Chem.* 261:5334–5340.

Maloney, K. M., M. Grandbois, C. Salesse, D. W. Grainger, and M. Roberts. 1995. Phospholipase A_2 domain formation in hydrolysed asymmetric phospholipid monolayers at the air-water interface. *Biochim. Biophys. Acta.* 1235:395–405.

Mou, J., J. Yang, C. Huang, and Z. Shao. 1994a. Alcohol induces interdigitated domains in unilamellar phosphatidylcholine bilayers. *Biochemistry.* 33:9981–9985.

Mou, J., J. Yang, and Z. Shao. 1994b. Tris(hydroxymethyl)aminomethane ($C_4H_{11}NO_3$) induced a ripple phase in supported unilamellar phospholipid bilayers. *Biochemistry.* 33:4439–4443.

Müller, D. J., C.-A. Schoenenberger, G. Büldt, and A. Engel. 1996. Immune-atomic force microscopy of purple membrane. *Biophys. J.* 70:1796–1802.

Okahata, Y., and Y. Ebara. 1992. Observation of phospholipase A_2 activity towards the hydrolysis of phospholipid Langmuir-Blodgett films deposited on a quartz microbalance. *J. Chem. Soc. Chem. Commun.* N2: 117–117.

op den Kamp, J. A., M. T. Kauerz, and L. L. v. Deenen. 1975. Action of pancreatic phospholipase A_2 on phosphatidylcholine bilayers in different physical states. *Biochim. Biophys. Acta.* 406:169–177.

Patil, G. S., R. H. Matthews, and D. G. Cornwell. 1973. Kinetics of the processes of desorption from fatty acid monolayers. *J. Lipid. Res.* 14:26–31.

Radmacher, M., M. Fritz, H. G. Hansma, and P. K. Hansma. 1994. Direct observation of enzyme activity with the atomic force microscope. *Science.* 265:1577–1579.

Radmacher, M., M. Fritz, and P. K. Hansma. 1995. Measuring the elastic properties of biological materials with the atomic force microscope. *Biophys. J.* 68:A139.

Radmacher, M., R. W. Tillmann, M. Fritz, and H. E. Gaub. 1992. From molecules to cells—imaging soft samples with the AFM. *Science.* 257: 1900–1905.

Reynolds, L. J., W. N. Washburn, R. A. Deems, and E. A. Dennis. 1991. Assay strategies and methods for phospholipases. *Methods Enzymol.* 197:3–23.

Rief, M., M. Gautel, F. Oesterhelt, J. M. Fernandez, and H. E. Gaub. 1997. Reversible unfolding of individual titin Ig-domains by AFM. *Science.* 276:1109–1112.

Shao, Z., and J. Yang. 1995. Progress in high resolution atomic force microscopy in biology. *Q. Rev. Biophys.* 28:195–251.

Speijer, H., P. L. A. Giesen, R. F. A. Zwall, C. E. Hanck, and W. T. Hermens. 1996. Critical micelle concentrations and stirring are rate-limiting in the loss of lipid mass during membrane degration by phospholipase A_2. *Biophys. J.* 70:2239–2247.

Tamm, L. K., and H. M. McConnell. 1985. Supported phospholipid bilayers. *Biophys. J.* 47:105–113.

van Hoogevest, P., J. de Gier, and B. de Kruijff. 1984. Determination of the size of the packing defects in dimyristoylphosphatidylcholine bilayer present at the phase transition temperature. *FEBS Lett.* 171:160–164.

Verger, R., M. C. E. Mieras, and G. H. de Haas. 1973. Action of phospholipase A at interfaces. *J. Biol. Chem.* 248:4023–4034.

Verger, R., and C. Rivière. 1987. Les enzymes lipolytiques: une étude cinétique. *Rev. Fr. Corps Gras.* 1:7–13.

Vernon, L. P., and J. D. Bell. 1992. Membrane structure toxins and phospholipase A_2 activity. *Pharmacol. Ther.* 54:269–295.

Wendel, M., H. Lorenz, and J. P. Kotthaus. 1995. Sharpened electron beam deposited tips for high resolution atomic force microscope lithography and imaging. *Appl. Phys. Lett.* 67:3732–3734.